Technical article

The Anatomy of Negative Refraction

Abstract — The mechanism of negative refraction (electromagnetic waves bending the 'wrong' way at material interfaces) and the closely related phenomenon of backward waves (phase velocity opposite to group velocity) are examined. It is shown that in periodic dielectric structures, such as metamaterials and photonic crystals, backward waves disappear in the homogenization limit, when the lattice cell size becomes negligible relative to the vacuum wavelength. The paper establishes a lower bound for the cell size of metamaterials capable of supporting backward waves. Introductory material and historical notes are included.
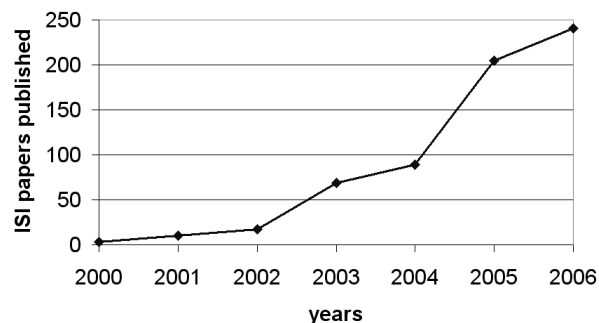
Figure 1: Number of ISI papers published on negative refraction. (ISI database query: "negative refraction" OR "negative index" material OR "double-negative" material.)

I INTRODUCTION

Negative refraction (electromagnetic waves bending the 'wrong' way at material interfaces) and the closely related phenomenon of backward waves (phase velocity opposite to group velocity) have become one of the most intriguing areas of research in nanophotonics this century, with thousands of research papers published and a number of books and review papers readily available: P.W. Milonni [20], G.V. Eleftheriades & K.G. Balmain (eds.) [7], S.A. Ramakrishna [33], J.B. Pendry & D.R. Smith [31], and others. The annual numbers of ISI publications (Fig. 1) illustrate the rapidly rising interest in this subject. Negative refraction being an odd phenomenon, it is perhaps fitting that the production of papers is above the average trend in odd years.

The objective of this paper is three-fold: (i) to clarify the mechanism of negative refraction and backward waves in periodic structures; (ii) to examine whether the 'metamaterial' and 'photonic crystal' species of negative refraction are fundamentally different; (iii) to show that backward waves disappear in the homogenization limit and to establish a lower bound for the lattice cell size of materials capable of supporting backward waves. Much of the introductory and background material in this paper is drawn from the upcoming book [49]; however, the main results related to the minimum lattice cell size are new.

Over 60 years ago, L.I. Mandelshtam in his lecture notes [17, 18] pointed out that waves would refract negatively at an interface boundary between a regular and a backward-wave medium. In his 1967 paper [50],[1] V.G. Veselago showed that waves in materials with simultaneously negative dielectric permittivity ϵ and magnetic permeability μ would exhibit quite unusual behavior of propagation and refraction. More specifically:

- Vectors $\mathbf{E}$, $\mathbf{H}$ and $\mathbf{k}$, in that order, form a left-handed system. Consequently, the Poynting vector $\mathbf{E} \times \mathbf{H}$ and the wave vector $\mathbf{k}$ have opposite directions.

- The Doppler and Vavilov-Cerenkov effects are 'reversed'. The sign of the Doppler shift in frequency is opposite to what it would be in a regular material. The Poynting vector of the Cerenkov radiation forms an obtuse angle with the direction of motion of a superluminal particle in a medium, while the wave vector of the radiation is directed *toward* the trajectory of the particle.

- Light propagating from a regular medium into a double-negative material bends "the wrong way" (Fig. 2). In Snell's law, this corresponds to a negative index of refraction.

- A slab with $\epsilon = -1$, $\mu = -1$ in air acts as an unusual lens (Fig. 3).[2]

Subjects closely related to Veselago's work had in fact been discussed in the literature well before his seminal publication – as early as in 1904. S.A. Tretyakov [47], C.L. Holloway *et al.* [9] and A. Moroz[3] provide the following references:

- A 1904 paper by H. Lamb [11] on waves in mechanical (rather than electromagnetic) systems.

- A. Schuster's monograph [35], pp. 313–318; a 1905 paper by H.C. Pocklington [32].

- L.I. Mandelshtam's short paper [16] and, even more importantly, his lectures on negative refraction and backward waves [17, 18] (more than two decades prior to Veselago's work, as already noted in the introductory paragraphs. Mandelshtam's 1945 paper, but not the lecture notes, is cited by Veselago.)

- A number of papers in Russian technical journals from the 1940s to the 1970s: by D.V. Sivukhin (1957) [40], V.E. Pafomov (1959) [26] and R.A. Silin (1959, 1978) [38, 39]. Silin's earlier review paper (1972) [39], where he focuses on wave propagation in artificial periodic structures.

In one of his lectures cited above, Mandelshtam writes, in reference to a figure similar to Fig. 2 ([18], pp. 464–465):[4]

> "... at the interface boundary the tangential components of the fields ... must be continuous. It is easy

---

[1]Published in 1967 in Russian. In the English translation that appeared in 1968, the original Russian paper in mistakenly dated as 1964.

[2]V.G. Veselago remarks that this is not a lens 'in the usual sense of the word' because it does not focus a parallel beam to a point.

[3]http://www.wave-scattering.com/negative.html

[4]My translation from the Russian. A similar quote is given by S.A. Tretyakov in [47].
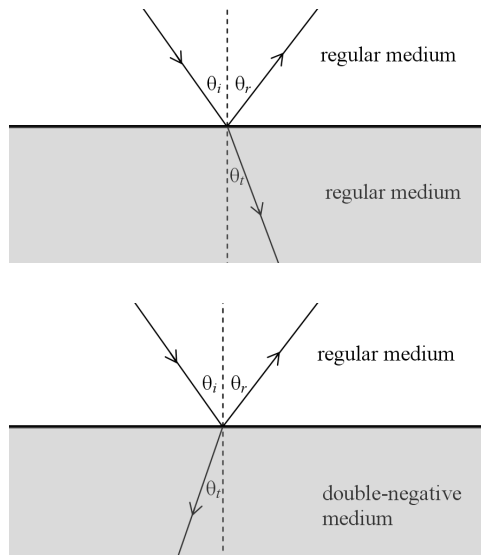
Figure 2: At the interface between a regular medium and a double-negative medium light bends "the wrong way"; in Snell's law, this implies a negative index of refraction. Arrows indicate the direction of the Poynting vector that in the double-negative medium is opposite to the wave vector.
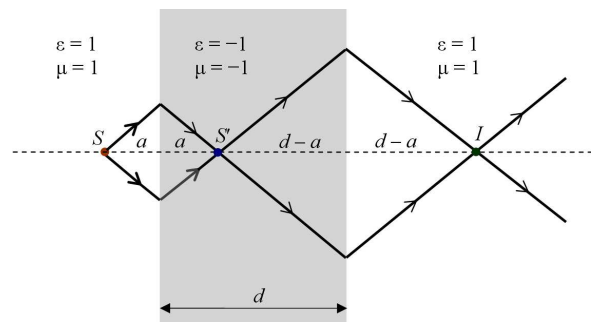

Figure 3: The Veselago slab of a double-negative material acts as an unusual lens. Due to the negative refraction at both surfaces of the slab, a point source S located at a distance $a < d$ has a virtual image S' inside the slab and a real image I outside. The arrows indicate the direction of the Poynting vector, not the wave vector.

to show that these conditions cannot be satisfied with a reflected wave (or a refracted wave) alone. But with both waves present, the conditions can always be satisfied. From that, by the way, it does not at all follow that there must only be *three* waves and not more: the boundary conditions do allow one more wave, the fourth one, traveling at the angle $\pi - \phi_1$ in the second medium. Usually it is tacitly assumed that this fourth wave does not exist, i.e. it is postulated that only one wave propagates in the second medium.

... [the law of refraction] is satisfied at angle ϕ_1 as well as at $\pi - \phi_1$. The wave ... corresponding to ϕ_1 moves away from the interface boundary. ... The wave corresponding to $\pi - \phi_1$ moves toward the interface boundary. It is considered self-evident that the second wave cannot exist, as light impinges from the first medium onto the second one, and hence in the second medium *energy* must flow away from the interface boundary. But what does energy have to do with this? The direction of wave propagation is in fact determined by its *phase* velocity, whereas energy moves with *group* velocity. Here therefore there is a logical leap that remains unnoticed only because we are accustomed to the coinciding directions of propagation of energy and phase. If these directions do coincide, i.e. if group velocity is positive, then everything comes out correctly. If, however, we are dealing with the case of negative group velocity – quite a realistic case, as I already said, – then everything changes. Requiring as before that energy in the second medium flow *away* from the interface boundary, we arrive at the conclusion that phase must run toward this boundary and, therefore, the direction of propagation of the refracted wave will be at the $\pi - \phi_1$ angle to the normal. However unusual this setup may be, there is, of course, nothing surprising about it, for phase velocity does not tell us anything about the direction of energy flow."

Of the earlier contributions to the subject, a notable one was made by R. Zengerle in his PhD thesis on singly and doubly periodic waveguides in the late 1970s. His journal publication of 1987 [54] contains, among other things, a subsection entitled "Simultaneous positive and negative ray refraction". Quote:

"Figure 10 shows refraction phenomena in a periodic waveguide whose effective index ... in the modulated region is ... higher than ... in the unmodulated region. The grating lines, however, are not normal to the boundaries. As a consequence of the boundary conditions, two Floquet-Bloch waves corresponding to the upper and lower branches of the dispersion contour ... are excited simultaneously ... resulting generally in two rays propagating in different directions. This ray refraction can be described by two effective ray indices: one for ordinary refraction ... and the other ... with a negative refraction angle ... "

Similar observations are made in Silin's 1972 paper [39]; see also a quote in [49].

A turning point in the research on double-negative materials came in 1999–2000, when J.B. Pendry *et al.* [30] showed theoretically, and D.R. Smith *et al.* [45] confirmed experimentally, negative refraction in an artificial material with split-ring resonators. A further discovery was made by Pendry in his 'perfect lens' paper in 2000 [29]. While Veselago's description of his 'lens' relied purely on geometric optics, Pendry's electromagnetic analysis showed that the evanescent part of light emitted by the source is *amplified* by the slab, with the ultimate result of perfect transmission and focusing of both propagating and evanescent components of the wave.

The first publication on what today would be called a (quasi)-perfect cylindrical lens was a 1994 paper by N.A. Nicorovici *et al.* [24] (now more detailed follow-up papers by G.W. Milton *et al.* [22, 21] are available).[5] These authors considered a coated dielectric cylinder, with the core of radius r_{core} and permittivity ϵ_{core}, the shell (coating) with the outer radius r_{shell} and permittivity ϵ_{shell} – embedded in a background medium with permittivity ϵ_{bg}. It turns out, first, that such a coated cylinder is completely transparent to the outside H-mode field (the H-field along the axis of the cylinder) under the quasistatic

---

[5] I am grateful to N.-A. Nicorovici and G.W. Milton for pointing these contributions out to me.

approximation if $\epsilon_{\rm core} = \epsilon_{\rm bg} = 1$, $\epsilon_{\rm shell} \rightarrow -1$. (The limiting case $\epsilon_{\rm shell} \rightarrow -1$ should be interpreted as the imaginary part of the permittivity tending to zero, while the real part is fixed at -1: $\epsilon_{\rm shell} = -1 - {\rm i}\epsilon''_{\rm shell}$, $\epsilon''_{\rm shell} \rightarrow 0$.)[6] Second, under these conditions for the dielectric constants, many unusual imaging properties of coated cylinders are observed. For example, a line source placed outside the coated cylinder at a radius $r_{\rm src} < r^3_{\rm shell}/r^2_{\rm core}$ would have an image *outside* the cylinder, at $r_{\rm image} = r^4_{\rm shell}/(r^2_{\rm core} r_{\rm src})$.

Truly homogeneous materials, in the Veselago sense, are not currently known and could be found in the future only if some new molecular-scale magnetic phenomena are discovered. Consequently, much effort has been devoted to the development of artificial metamaterials capable of supporting backward waves and producing negative refraction. Selected developments are as follows (all numbers approximate): D.R. Smith *et al.* [45] (copper split-ring resonators (SRR) and wires, 4.85 GHz, 2000); R.A. Shelby *et al.* [37] (copper SRR and strips, 10 GHz, 2001); C.G. Parazzoli *et al.* [27] (a stack of SRRs with metal strips, 12.6 GHz, 2003); A.A. Houck *et al.* [10] (composite wire and SRR prisms, 10 GHz, 2003); D.R. Smith & D.C. Vier [43] (copper SRR and strips, 11 GHz, 2004); V.M. Shalaev *et al.* [36] (pairs of nanorods, 200 THz, 2006); S. Zhang *et al.* [55] (nano-fishnet with elliptical voids, 170 THz, 2006); G. Dolling *et al.* [6, 5] (nano-fishnet with rectangular voids, 210 THz, 380 THz, 2006–07).

In these designs, the cell size as a fraction of the vacuum wavelength varies between ∼0.11–0.42. Could further improvements in nanofabrication and design bring the cell size down to a small fraction of the wavelength, thereby approaching the Veselago case of a homogeneous material? This question will become central in Section IX.

Separately from the progress in metamaterials, negative refraction was observed and analyzed in singly and doubly periodic waveguides (R. Zengerle [54], late 1970s – 1980s) and in photonic crystals (M. Notomi [25] in 2000). Since 2000, there have been a number of publications on negative refraction and the associated lensing effects in photonic crystals: C. Luo *et al.* [15], "all-angle negative refraction" in a bcc lattice of air cubes in a dielectric; E. Cubukcu *et al.* [3], experimental and theoretical demonstration of negative refraction and superlensing in a 2D photonic crystal in the microwave range; R. Moussa *et al.* [23], experimental and theoretical study of negative refraction and superlensing in a triangular array of rectangular dielectric bars; V. Yannopapas & A. Moroz [52] and M.S. Wheeler *et al.* [51], negative refraction in a lattice of polaritonic spheres S. Foteinopoulou & C.M. Soukoulis, a general analysis of negative refraction at the air-crystal interfaces, with Notomi's example as a specific case (a 2D hexagonal lattice of rods with permittivity 12.96 and the radius of 0.35 lattice size). See also P.V. Parimi *et al.* [28] (left-handed behavior of the waves in a triangular lattice of cylindrical copper rods). An example due to R. Gajic, R. Meisels *et al.* [8, 19] is discussed in subsequent Sections.

All these intriguing findings have led to the *presumption that there are two species of negative refraction*, one occurring in photonic crystals and another one in metamaterials. The latter are viewed as conceptually close to the ideal homogeneous "Veselago medium". There are, indeed, obvious differences between these two cases in terms of the underlying structure, composition and fabrication (e.g. lossless dielectric spheres vs. lossy metallic inclusions such as split ring resonators, pairs of

nanorods, fishnets, etc.) On a more fundamental level, however, all cases can be characterized by a periodically varying complex dielectric function $\epsilon(\mathbf{r})$, and it is legitimate to ask if there might be any *principal* difference between metamaterials and crystals.

Importantly, can metamaterials, as a matter of principle, be (arbitrarily) close to an ideal Veselago medium? A key point of this paper is that periodic dielectric structures that support backward waves cannot have arbitrarily small lattice cells; there is a fundamental lower bound on the cell size as a fraction of the free-space wavelength.

The remainder of the paper is organized as follows. First, following V.G. Veselago, Section II examines wave propagation in a (hypothetical) medium with simultaneously negative ϵ and μ. Sections III–V provide background information on the governing equations, as well as on Bloch waves and their properties. The Fourier-space formulation of the electromagnetic problem is given in Section VI. Mandelshtam's interesting examples of backward waves – one mechanical and one electromagnetic – are presented in Sections VII and VIII. Finally, Section IX poses and answers a new question: are there two separate species of negative refraction?

II FORWARD AND BACKWARD PLANE WAVES IN A HOMOGENEOUS ISOTROPIC MEDIUM

In backward waves, energy and phase propagate in opposite directions. Let us first examine this counterintuitive phenomenon in a hypothetical homogeneous isotropic medium with unusual material parameters (the "Veselago medium"). In subsequent Sections, we shall turn to the analysis of forward and backward *Bloch* waves in periodic dielectric structures.

Consider the behavior of plane waves in a homogeneous isotropic medium with arbitrary constant complex parameters ϵ and μ at a given frequency. The only stipulation is that the medium be passive (no generation of energy), which under the $\exp(+{\rm i}\omega t)$ phasor convention implies negative imaginary parts ϵ'' and μ'' of ϵ and μ. It will be helpful to assume that these imaginary parts are *strictly negative* and to view lossless materials as a limiting case of small losses: $\epsilon'' \rightarrow -0$, $\mu'' \rightarrow -0$. The goal is to establish conditions for the plane wave to be forward or backward. In the latter case, one has a "Veselago medium".

Let the plane wave propagate along the x axis, with $E = E_y$ and $H = H_z$. Then we have

$$E = E_y = E_0 \exp(-{\rm i}kx) \tag{1}$$

$$H = H_z = H_0 \exp(-{\rm i}kx) \tag{2}$$

where E_0, H_0 are some complex amplitudes. It immediately follows from Maxwell's equations that

$$H_0 = \frac{k}{\omega\mu} E_0 \tag{3}$$

$$k = \omega\sqrt{\mu\epsilon} \quad \text{(which branch of the square root?)} \tag{4}$$

Which branch of the square root "should" be implied in the formula for the wavenumber? In an unbounded medium, there is complete symmetry between the $+x$ and $-x$ directions, and waves corresponding to both branches of the root are equally valid. It is clear, however, that each of the waves is unbounded in one of the directions, which is not physical.

For a more physical picture, it is tacitly assumed that the unbounded growth is truncated: e.g. the medium and the wave occupy only half of the space, where the wave decays. With this

---

[6]The $\exp(+{\rm i}\omega t)$ convention is used for complex phasors.

in mind, let us focus on one of the two waves – say, the one with a negative imaginary part of k:

$$k'' \; < \; 0 \qquad (5)$$

(The analysis for the other wave is completely analogous.) Splitting up the real and imaginary exponentials

$$\exp(-ikx) \; = \; \exp(-i(k' + ik'')x) \; = \; \exp(k''x)\exp(-ik'x)$$

we observe that this wave decays in the $+x$ direction. On physical grounds, one can argue that energy in this wave must flow in the $+x$ direction as well. This can be verified by computing the time-averaged Poynting vector

$$P \; = \; P_x \; = \; \frac{1}{2}\operatorname{Re} E_0 H_0^* \; = \; \frac{1}{2}\operatorname{Re}\frac{k}{\omega\mu}|E_0|^2 \qquad (6)$$

To express P via material parameters, let

$$\epsilon = |\epsilon|\exp(-i\phi_\epsilon); \quad \mu = |\mu|\exp(-i\phi_\mu); \quad 0 < \phi_\epsilon, \phi_\mu < \pi$$

Then the square root with a negative imaginary part, consistent with the wave (5) under consideration, gives

$$k \; = \; \omega\sqrt{|\mu|\,|\epsilon|}\exp\left(-i\,\frac{\phi_\epsilon + \phi_\mu}{2}\right) \qquad (7)$$

Ignoring all positive real factors irrelevant to the sign of P in (6), we get

$$\operatorname{sign} P \; = \; \operatorname{sign}\operatorname{Re}\frac{k}{\mu} \; = \; \operatorname{sign}\cos\frac{\phi_\epsilon - \phi_\mu}{2}$$

The cosine, however, is always positive, as $0 < \phi_\epsilon, \phi_\mu < \pi$. Thus, as expected, P_x is positive, indicating that energy flows in the $+x$ direction indeed.

The type of the wave (forward vs. backward) therefore depends on the sign of phase velocity ω/k' – that is, on the sign of k'. As follows from (7),

$$\operatorname{sign} k' \; = \; \operatorname{sign}\cos\frac{\phi_\epsilon + \phi_\mu}{2}$$

and the wave is backward if and only if the cosine is negative, or

$$\phi_\epsilon + \phi_\mu \; > \; \pi \qquad (8)$$

An algebraically equivalent criterion can be derived by noting that the cosine function is monotonically decreasing on $[0, \pi]$ and hence $\phi_\epsilon > \pi - \phi_\mu$ is equivalent to

$$\cos\phi_\epsilon \; < \; \cos(\pi - \phi_\mu)$$

or

$$\cos\phi_\epsilon \; + \; \cos\phi_\mu \; < \; 0$$

This coincides with the Depine-Lakhtakia condition [4] for backward waves:

$$\frac{\epsilon'}{|\epsilon|} \; + \; \frac{\mu'}{|\mu|} \; < \; 0 \qquad (9)$$

This last expression is invariant with respect to complex conjugation and is therefore valid for both phasor conventions $\exp(\pm i\omega t)$.

Note that the analysis above relies only on Maxwell's equations and the definitions of the Poynting vector and phase velocity. No considerations of causality, so common in the literature on negative refraction, were needed to establish the backward-wave conditions (8), (9).

III FIELD EQUATIONS AND BLOCH WAVES

We shall consider the usual 1D, 2D and 3D renditions of time-harmonic Maxwell's equations. At optical frequencies, the intrinsic permeability of all media can be set to μ_0 (L.D. Landau and E.M. Lifshitz [12], §60).[7]

In 1D, the equation for the E field is

$$E''(x) \; + \; k^2 E(x) \; = \; 0, \quad \text{with } k^2 = \omega^2\mu_0\epsilon(x) \qquad (10)$$

In periodic structures, with ϵ a periodic function of x, a fundamental solution of the above equation is the Bloch-Floquet wave of the form

$$E(x) \; = \; E_{\text{PER}}(x)\exp(-iK_B x); \qquad (11)$$

where K_B is the Bloch wavenumber and subscript 'PER' marks periodic functions with a given spatial period a (the lattice cell size).

In 2D, the E-mode (one-component field $E = E_z$) is described by the equation

$$\nabla^2 E \; + \; k^2 E \; = \; 0, \quad \text{with } k^2 = \omega^2\mu_0\epsilon(x, y) \qquad (12)$$

Again, if ϵ is a periodic function of coordinates, the fundamental solutions of the field equation are known to be Bloch waves with a (yet undetermined) wave vector $\mathbf{K}_B = (K_x, K_y)$:

$$E(\mathbf{r}) \; = \; E_{\text{PER}}(\mathbf{r})\exp(-i\mathbf{K}_B \cdot \mathbf{r}); \quad \mathbf{r} \equiv (x, y), \qquad (13)$$

Assuming for simplicity a square lattice cell of size a, subscript 'PER' implies periodicity with respect to any lattice vector $(n_x a, n_y a)$ with integer n_x, n_y.

The governing equation for the H-mode (one-component H-field) is

$$\nabla \cdot \epsilon^{-1}\nabla H \; + \; \omega^2\mu_0 H \; = \; 0 \qquad (14)$$

and the expression for the Bloch H-wave is completely analogous to (13).

Finally, the 3D E-field equation and the corresponding Bloch wave can be written as

$$\nabla \times \nabla \times \mathbf{E} \; - \; k^2\mathbf{E} \; = \; 0, \qquad (15)$$

$$E(\mathbf{r}) \; = \; E_{\text{PER}}(\mathbf{r})\exp(-i\mathbf{K} \cdot \mathbf{r}); \qquad (16)$$

$$\mathbf{r} \equiv (x, y, z), \quad \mathbf{K}_B = (K_x, K_y, K_z)$$

The governing equation for the H field is

$$\nabla \times \epsilon^{-1}\nabla \times \mathbf{H} \; - \; \omega^2\mu_0\mathbf{H} \; = \; 0 \qquad (17)$$

IV FOURIER HARMONICS OF BLOCH WAVES

In 1D, the periodic factor $E_{\text{PER}}(x)$ (11) can be expanded into a Fourier series with coefficients e_m ($m = 0, \pm 1, \pm 2, \ldots$)

$$E(x) \; = \; \sum_{m=-\infty}^{\infty} e_m\exp(im\kappa_0 x)\exp(-iK_B x), \quad \kappa_0 = 2\pi a^{-1} \qquad (18)$$

The Fourier coefficients e_m are given by the usual integral expressions

$$e_m \; = \; a^{-1}\int_a E_{\text{PER}}(x)\exp(-im\kappa_0 x)\,dx \qquad (19)$$

---

[7]Artificial magnetism can be created in periodic dielectric structures at optical frequencies (W. Cai *et al.* [2], S. Linden *et al.* [13]). The equivalent 'mesoscopic' permeability may then be different from μ_0, but the intrinsic *microscopic* permeability of the materials involved is still μ_0.

where the integration is over any period of length a.

Similarly, in 2D the Fourier series for $\mathbf{E}_{\text{PER}}(x,y)$ has the form

$$\mathbf{E}_{\text{PER}}(\mathbf{r}) = \sum_{\mathbf{m} \in \mathbb{Z}^2} \tilde{e}_{\mathbf{m}} \exp(i\mathbf{k_m} \cdot \mathbf{r}), \qquad (20)$$

$$\mathbf{k_m} = 2\pi a^{-1} \mathbf{m} \equiv 2\pi a^{-1} (m_x, m_y)$$

with integers m_x, m_y. A square lattice is assumed for simplicity; $\tilde{e}_{\mathbf{m}}$ are the Fourier coefficients. The field is treated as vectorial for generality, even if it happens to have only one Cartesian component. The Bloch wave is obtained by multiplying $\mathbf{E}_{\text{PER}}$ with the Bloch exponential:

$$\mathbf{E}(\mathbf{r}) = \sum_{\mathbf{m} \in \mathbb{Z}^3} \mathbf{E_m} \equiv \sum_{\mathbf{m} \in \mathbb{Z}^3} \mathbf{e_m} \exp(i\mathbf{k_m} \cdot \mathbf{r}) \exp(-i\mathbf{K}_B \cdot \mathbf{r}) \qquad (21)$$

This representation of the Bloch wave as a suite of plane waves $\mathbf{E}_m$ is essential for the analysis and physical interpretation of energy flow, phase velocity and other properties of this wave (B. Lombardet *et al.* [14]).

For $\mu = \mu_0$, the above expression for $\mathbf{E}(\mathbf{r})$ leads, via the Maxwell $\nabla \times \mathbf{E}$ equation, to a similar decomposition of the magnetic field:

$$\mathbf{H}(\mathbf{r}) = \sum_{\mathbf{m} \in \mathbb{Z}^3} \mathbf{H_m} \equiv \sum_{\mathbf{m} \in \mathbb{Z}^3} \mathbf{h_m} \exp(i\mathbf{k_m} \cdot \mathbf{r}) \exp(-i\mathbf{K}_B \cdot \mathbf{r}), \qquad (22)$$

$$\mathbf{h_m} = \frac{\mathbf{k_m}}{\omega \mu_0} \mathbf{e_m}$$

It is important to note from the outset, as Lombardet *et al.* do in [14], that the individual plane-wave components of the Bloch wave do not satisfy Maxwell's equations in the periodic medium and therefore do not represent physical fields. Only taken together do these Fourier harmonics form a valid field.

It is straightforward to verify that the plane waves in the decomposition are orthogonal functions (in the sense of standard vector $\mathbf{L}_2$ inner product) over the lattice cell. Hence, by Parseval's theorem, the time- and cell-averaged Poynting vector $< \mathbf{P} > = < \text{Re}\{\mathbf{E} \times \mathbf{H}^*\} > /2$ can be represented as a sum of the Poynting vectors for the individual plane waves (B. Lombardet *et al.* [14]):

$$< \mathbf{P} > = \sum_{\mathbf{m} \in \mathbb{Z}^3} \mathbf{P_m}; \quad \mathbf{P_m} = \frac{k_m}{2\omega\mu_0} |\mathbf{e_m}|^2 \qquad (23)$$

Next, group velocity $\partial\omega/\partial k$ is clearly the same for all plane wave components, and hence group velocity for the whole Bloch wave can be defined as

$$v_g = \frac{\partial\omega}{\partial K_B} \qquad (24)$$

In cases of weak dispersion, it can be shown [53, 49] that this velocity, indeed, approximately represents signal velocity in the periodic medium.

V   Intrinsic and Extrinsic Properties

For the analysis of anomalous wave propagation and refraction, it is important to distinguish *intrinsic* and *extrinsic* characteristics of the wave. Intrinsic properties of the wave refer to its characterization as either forward or backward; that is, whether the Poynting vector and phase velocity (if it can be properly defined) are in the same or opposite directions. (Or, more generally, at an acute or obtuse angle.) Extrinsic properties refer to conditions at the interface of the periodic structure with air or another homogeneous medium. A key point is that refraction at the interface depends not only on the intrinsic characteristics of the wave in the bulk, but also on the way the Bloch wave is excited [14].

This can be explained as follows. Let the x axis run along the interface boundary between air and a material with an a-periodic permittivity $\epsilon(x)$. For simplicity, we assume that ϵ does not vary along the normal coordinate y. Such a periodic medium can support Bloch E-modes of the form

$$E(\mathbf{r}) = \sum_{m=-\infty}^{\infty} e_m \exp(im\kappa_0 x) \exp(-iK_{Bx}x) \exp(-iK_y y)$$

Let the first-Brillouin-zone harmonic ($m = 0$) have an appreciable magnitude e_0, thereby defining phase velocity ω/K_{Bx} in the x-direction. For $K_{Bx} > 0$, this velocity is positive.

But any plane-wave component of the Bloch wave can serve as an 'excitation channel'[8] for this wave, provided that – for a certain angle of incidence – it matches the x-component of the incident wave in the air:

$$K_{Bx} - \kappa_0 m = k_x^{\text{air}}$$

This will correspond to a propagating, rather than evanescent, wave in the air if $|K_{Bx} - \kappa_0 m| < k^{\text{air}}$.

First, suppose that the 'main' channel ($m = 0$) is used, so that $K_{Bx} = k_x^{\text{air}}$. If the Bloch wave in the material is a forward one, then the y-components of the Poynting vector P_y and the wave vector K_y are both directed *away* from the interface, and the usual positive refraction occurs. If, however, the wave is backward, then K_y is directed *toward* the surface (against the Poynting vector) and it can easily be seen that refraction is negative. This is completely consistent with Mandelshtam's original explanation.

Exactly the opposite occurs if the Bloch wave is excited through an excitation channel where $K_{Bx} - \kappa_0 m$ is negative (say, for $m = 1$). The matching condition at the interface then implies that the x-component of the wave vector in the air is negative in this case. Repeating the argument of the previous paragraph, one discovers that for a *forward* Bloch wave refraction is now *negative*, while for a backward wave it is positive.

In summary, refraction properties at the interface are a function of the intrinsic characteristics of the wave in the bulk *as well as* the excitation channel, with four substantially different combinations possible. This conclusion summarizes the results already available but dispersed in the literature [1, 14, 8].

VI   Fourier-Space Equations

Fourier analysis (Plane Wave Expansion, PWE) is the most common way to analyze and compute the band structure in any number of dimensions. The method is very well known and is described here briefly to make the paper self-contained.

Let us start with the 1D case. For simplicity of exposition, let us assume a lossless nonmagnetic periodic medium, where the electric field $E = E_y(x)$ is governed by the wave equation (10); ϵ is assumed to be an a-periodic function. We are looking for a solution in the form of the Bloch-Floquet wave (11), with $E_{\text{PER}}(x)$ and K_B to be determined.

To Fourier-transform the wave equation (10), one expresses the dielectric permittivity via a Fourier series with coefficients $\tilde{\epsilon}_m$:

$$\epsilon(x) = \sum_{m=-\infty}^{\infty} \tilde{\epsilon}_m \exp(im\kappa_0 x) \qquad (25)$$

_____

[8] A lucid term due to B. Lombardet *et al.* [14].

In Fourier space, multiplication $\epsilon(x)E(x)$ (i.e. multiplication of the Fourier series (18) and (25)) turns into convolution and the problem becomes

$$\mathcal{K}^2 \underline{e} = \omega^2 \mu_0 \, \Xi \underline{e} \qquad (26)$$

Here $\underline{e} = (\ldots, e_{-2}, e_{-1}, e_0, e_1, e_2, \ldots)^T$ is the (infinite) column vector of Fourier coefficients of the field; $\mathcal{K}$ is an infinite diagonal matrix with the entries $k_m = K_B - \kappa_0 m$, or equivalently

$$\mathcal{K} = K_B I - \kappa_0 N, \qquad (27)$$

where I is the identity matrix and

$$N = \begin{pmatrix} \ldots & \ldots & \ldots & \ldots & \ldots & \ldots & \ldots \\ \ldots & -2 & \ldots & \ldots & \ldots & \ldots & \ldots \\ \ldots & \ldots & -1 & \ldots & \ldots & \ldots & \ldots \\ \ldots & \ldots & \ldots & 0 & \ldots & \ldots & \ldots \\ \ldots & \ldots & \ldots & \ldots & 1 & \ldots & \ldots \\ \ldots & \ldots & \ldots & \ldots & \ldots & 2 & \ldots \\ \ldots & \ldots & \ldots & \ldots & \ldots & \ldots & \ldots \end{pmatrix} \qquad (28)$$

Finally, matrix Ξ in (26) is composed of the Fourier coefficients of ϵ:

$$\Xi_{ml} = \epsilon_{m-l} \qquad (29)$$

for any row m and column l ($-\infty < m, l < \infty$).

The infinite-dimensional eigenproblem (26) must in practice be truncated to a finite number of harmonics. The computational trade-off is clear: as the number of harmonics grows, both computational complexity and accuracy increase. This paper does not focus on the computational aspects of the problem but may have implications for the simulation and design of photonic structures.

The *2D case* is handled in a similar fashion. The dielectric permittivity $\epsilon(x, y)$ is a periodic function of coordinates and can be expanded into its Fourier series

$$\epsilon = \sum_{\mathbf{m} \in \mathbb{Z}^2} \tilde{\epsilon}_{\mathbf{m}} \exp\left(i \mathbf{k_m} \cdot \mathbf{r}\right) \qquad (30)$$

For the Bloch-Floquet E-field, the negative of the Laplace operator turns, in the Fourier domain, into multiplication with $|\mathbf{K}_B - \mathbf{k_m}|^2$. Further, the product $\epsilon \mathbf{E}$ of the wave equation turns into convolution, and thus the eigenvalue problem in Fourier space reads:

$$|\mathbf{k_n}|^2 e_{\mathbf{n}} = \omega^2 \mu_0 \sum_{\mathbf{m} \in \mathbb{Z}^2} \tilde{\epsilon}_{\mathbf{n-m}} e_{\mathbf{m}} \qquad (31)$$

This is an infinite set of equations for the eigenfrequencies and eigenmodes. As in 1D, for computational purposes, the system would need to be truncated to a finite size, but this matter is only tangential in the present paper. Fourier analysis of two- or three-component *vector* fields in periodic 2D or 3D structures is conceptually similar but technically more involved and is not included in this paper.

VII EXAMPLE: BACKWARD WAVES IN MANDELSHTAM'S CHAIN OF OSCILLATORS

This example, concerned with mechanical rather than electromagnetic waves, is interesting, instructive and has historical significance. Mandelshtam's four-page paper [16][9] published by his coworkers in 1945 after his death is very succinct, so a more

---

[9]The paper is also reprinted in Mandelshtam's lecture course [17].

detailed exposition below will hopefully prove useful. An electromagnetic analogy of this mechanical example (an optical grating) is the subject of the following Section.

Consider an infinite 1D chain of masses, with the nearest neighbors separated by an equilibrium distance d and connected by springs with a spring constant f. Newton's equation of motion for the displacement ξ_n of the nth mass m_n is

$$\ddot{\xi}(n) = \omega_n^2 \left[\xi(n-1) - 2\xi(n) + \xi(n+1)\right], \quad \omega_n^2 = \frac{f}{m_n} \quad (32)$$

For brevity, dependence of ξ on time is not explicitly indicated. For waves at a given frequency ω, switching to complex phasors yields

$$\omega^2 \xi(n) + \omega_n^2 \left[\xi(n-1) - 2\xi(n) + \xi(n+1)\right] = 0 \quad (33)$$

Mandelshtam considers *periodic* chains of masses, focusing on the case with just two alternating masses, m_1 and m_2. The discrete analog of the Bloch wave has the form

$$\xi(n) = \xi_{\text{PER}}(n) \exp(-iK_B nd) \qquad (34)$$

ξ_{PER} is a periodic function of n with the period of two and can hence be represented by a Euclidean vector $\underline{\xi} \equiv (a, b) \in \mathbb{R}^2$, where a and b are the values of $\xi_{\text{PER}}(n)$ for odd and even n, respectively.[10]

Substituting this discrete Bloch-type wave into the difference equation (33), we obtain

$$\begin{pmatrix} \omega_2^2(\lambda^2 + 1) & \lambda(\omega^2 - 2\omega_2^2) \\ \lambda(\omega^2 - 2\omega_1^2) & \omega_1^2(\lambda^2 + 1) \end{pmatrix} \begin{pmatrix} a \\ b \end{pmatrix} = 0, \quad (35)$$

$$\lambda \equiv \exp(-iK_B d)$$

Hence (a, b) is the null vector of the 2×2 matrix in the left hand side of (35). Equating the determinant to zero yields two eigenfrequencies $\omega_{\text{B1,B2}}$ of the Bloch wave

$$\omega_{\text{B1,B2}} = \omega_1^2 + \omega_2^2 \pm \lambda^{-1} \sqrt{(\omega_1^2 \lambda^2 + \omega_2^2)(\omega_2^2 \lambda^2 + \omega_1^2)}$$

To analyze group velocity of Bloch waves, compute the Taylor expansion of these eigenfrequencies around $K_B = 0$ (keeping in mind that $\lambda = \exp(-iK_B d)$):

$$\omega_{\text{B1}} = 2 \frac{d^2 \omega_2^2 \omega_1^2}{\omega_1^2 + \omega_2^2}$$

$$\omega_{\text{B2}} = 2(\omega_1^2 + \omega_2^2) - 2 \frac{d^2 \omega_2^2 \omega_1^2}{\omega_1^2 + \omega_2^2} K_B^2$$

which coincides with Mandelshtam's formulas at the bottom of p. 476 of his paper. Group velocity $v_g = \partial \omega_{\text{B}} / \partial K_B$ of long-wavelength Bloch waves is positive for the 'acoustic' branch ω_{B1} but negative for the 'optical' branch ω_{B2}.[11]

For $K_B = 0$ (i.e. $\lambda = 1$), simple algebra shows that the components of the second null vector $(a_{\text{B2}}, b_{\text{B2}})$ of (35) are proportional to the two particle masses:

$$\frac{a_{\text{B2}}}{b_{\text{B2}}} = -\frac{m_2}{m_1} \quad (K_B = 0) \qquad (36)$$

---

[10]Alternatively and equally well, ξ_{PER} can be represented via its two-term Fourier sum, familiar from discrete-time signal analysis:

$$\xi_{\text{PER}}(n) = \tilde{\xi}(0) + \tilde{\xi}(1) \exp(in\pi) = \tilde{\xi}(0) + (-1)^n \tilde{\xi}(1)$$

where $\tilde{\xi}(0) = \frac{1}{2}(\xi(0) + \xi(1)); \quad \tilde{\xi}(1) = \frac{1}{2}(\xi(0) - \xi(1))$

[11]On the acoustic branch, by definition, $\omega \to 0$ as $K_B \to 0$; on optical branches, $\omega \not\to 0$.

(The first null vector $a_{B1} = b_{B1}$ corresponding to the zero eigen-frequency for zero K_B represents just a translation of the chain as a whole and is uninteresting.)

Next, consider energy transfer along the chain. The force that mass $n-1$ exerts upon mass n is

$$F_{n-1,n} = [\xi(n-1) - \xi(n)] f$$

The mechanical 'Poynting vector' is the power generated by this force:

$$P_{n-1,n}(t) = F_{n-1,n}(t)\,\dot{\xi}(n,t)$$

the time average of which, via complex phasors, is

$$<P_{n-1,n}> = \frac{1}{2}\,\mathrm{Re}\,\{F_{n-1,n}\mathrm{i}\omega\xi(n)\}$$

For the 'optical' mode, i.e. the second eigenfrequency of oscillations, direct computation leads to Mandelshtam's expression

$$<P> = \frac{1}{2}\,f\omega ab\sin(K_B d)$$

The subscripts for $<P>$ have been dropped because the result is independent of n, as should be expected from physical considerations: no continuous energy accumulation occurs in any part of the chain.

We have now arrived at the principal point in this example. For small positive K_B ($K_B d \ll 1$), the Bloch wave has a long-wavelength component $\exp(-\mathrm{i}K_B nd)$. Phase velocity ω/K_B of the Bloch wave – in the sense discussed in more detail below – is positive. At the same time, the Poynting vector, and hence the group velocity, are negative because a_{B2} and b_{B2} have opposite signs in accordance with (36). Thus mechanical oscillations of the chain in this case propagate as a backward wave. An electromagnetic analogy of such a wave is mentioned very briefly in Mandelshtam's paper and is the subject of the following Section.

VIII   EXAMPLE: BACKWARD WAVES IN MANDELSHTAM'S GRATING

Let us assume a lossless nonmagnetic medium with 1D-periodic permittivity $\epsilon(x)$. The electric field $E = E_y(x)$ is governed by the wave equation (10). We are looking for a solution in the form of the Bloch-Floquet wave (11). Both $E_{\mathrm{PER}}(x)$ and K_B are *a priori* unknown and need to be determined. In Fourier space, $E_{\mathrm{PER}}(x)$ is given by its Fourier series (18) and ϵ is expressed via the Fourier series (25).

Mandelshtam's 1D volume grating mentioned in his paper [16] can, similarly to the chain of mechanical oscillators, support backward waves. For definiteness, let us assume a unit lattice cell and a sinusoidal variation of the permittivity:

$$\epsilon(x) = 2 + \cos 2\pi x = 2 + \frac{1}{2}\exp(\mathrm{i}2\pi x) + \frac{1}{2}\exp(-\mathrm{i}2\pi x)$$

Thus ϵ has only three nonzero Fourier coefficients: $\tilde{\epsilon}_{\pm 1} = 1/2$, $\tilde{\epsilon}_0 = 2$.

The eigenvalue problem (26), with the magnetic permeability normalized to unity for simplicity, is

$$\mathcal{K}^2\underline{e} = \omega^2\Xi\underline{e} \qquad (37)$$

The diagonal matrix $\mathcal{K}^2$ has entries

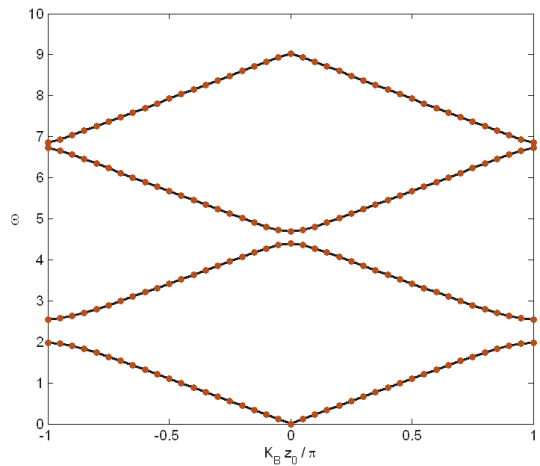$$\mathcal{K}_m^2 = (K_B - 2\pi m)^2, \quad m = 0, \pm 1, \pm 2, \ldots$$

Figure 4: The bandgap structure for the volume grating with $\epsilon(x) = 2 + \cos 2\pi x$. Solid line – $M = 5$ ($2 \times 5 + 1 = 11$ plane waves); circles – $M = 20$ ($2 \times 20 + 1 = 41$ plane waves).

and matrix Ξ is tridiagonal, with the entries in the mth row equal to

$$\Xi_{m,m} = \tilde{\epsilon}_0 = 2; \quad \Xi_{m\pm 1,m} = \tilde{\epsilon}_{\pm 1} = \frac{1}{2}$$

For any given value of the Bloch parameter K_B, numerical solution can be obtained by truncating the infinite system to the algebraic eigenvalue problem with $2M + 1$ equations ($m = -M, -M+1, \ldots M-1, M$).

The first four dispersion curves $\omega(K_B)$ are shown in Fig. 4; there are two frequency bandgaps in the figure, approximately [1.98, 2.55] and [4.40, 4.68], and infinitely many more gaps beyond the range of the chart. The numerical results are plotted for 41 equally spaced values of the normalized Bloch number $K_B a/\pi$ in $[-1, 1]$. There is no appreciable difference between the numerical results for $M = 5$ (11 equations) and $M = 20$ (41 equations). The high accuracy of the eigenfrequencies for a small number of plane waves in the expansion is due to the smooth variation of the permittivity. Discontinuities in ϵ would require a much higher number of harmonics.

In addition to the eigenvalues ω^2 of (37), the eigenvectors $\underline{e}$ are also of interest. As an example, let us set $K_B a = \pi/10$. Stem plots of the four eigenvectors corresponding to the four smallest eigenvalues $\omega^2 \approx 0.049, 18.29, 23.12$ and 77.83, are shown in Fig. 5. The first Bloch wave is almost a plane wave; the amplitudes of all harmonics other than e_0 are very small (but not zero, as it might appear from the figure); for example, $e_{-1} \approx 0.00057$, $e_1 \approx 0.00069$.

It is interesting to note that dispersion curves with positive and negative slopes $\partial\omega/\partial K_B$ (i.e. positive and negative group velocity) alternate in the diagram. Group velocity is positive for the lowest-frequency curve $\omega_1(K_B)$, negative for $\omega_2(K_B)$, positive again for $\omega_3(K_B)$, etc.

We now discuss the splitting of the Poynting vector into the individual 'Poynting components' $P_m = k_m|e_m|^2/(2\omega\mu)$ (23); this splitting has implications for the nature of the wave. The distribution of P_m for the first four Bloch modes in the grating is displayed in Fig. 6. The first mode shown in the upper left corner of the figure is almost a pure plane wave ($P_{\pm 1}$ are on the order of 10^{-5}; $P_{\pm 2}$ are on the order of 10^{-13}, and so on) and does not exhibit any unusual behavior.

Let us therefore focus on mode #2 (upper right corner of the figure). There are four non-negligible harmonics altogether. The stems to the right of the origin ($K > 0$) correspond to plane wave
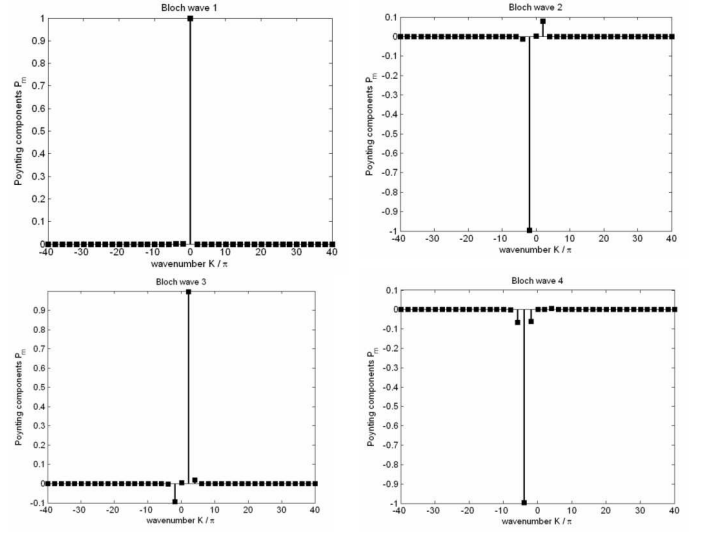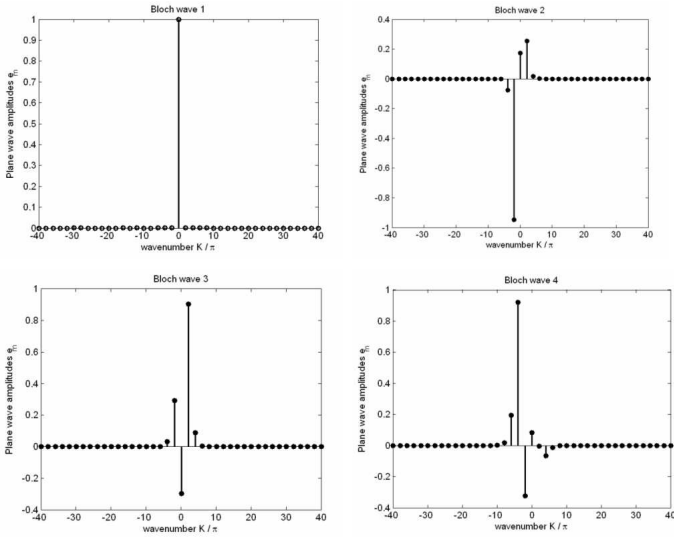
Figure 5: The amplitudes of the plane wave components of the first four Bloch waves for the volume grating with $\epsilon(x) = 2 + \cos 2\pi x$. Solution with 41 plane waves. $K_B a = \pi/10$.

Figure 6: The Poynting components P_m of the first four Bloch waves for the volume grating with $\epsilon(x) = 2 + \cos 2\pi x$. Solution with 41 plane waves. $K_B a = \pi/10$.

K/π	e_m	P_m
-5.9	-0.0023	$-1.79 \cdot 10^{-5}$
-3.9	-0.0765	-0.013
-1.9	-0.948	-0.997
0.1	**0.174**	**0.00177**
2.1	0.253	0.0783
4.1	0.0179	0.000767
6.1	0.000495	$8.73 \cdot 10^{-7}$

Table 1: The principal components of the second Bloch mode in the grating.

components propagating to the right, i.e. in the $+x$-direction. Stems to the left of the origin correspond to plane waves propagating to the left, and hence their Poynting values are negative. It is obvious from the figure that the negative components dominate and as a result power flows in the negative-x direction. The numerical values of the Poynting components and of the amplitudes of the plane wave harmonics are summarized in Table 1.

Now, the characterization of this wave as forward or backward hinges on the definition and sign of phase velocity. The smallest absolute value of the wavenumber in the Bloch 'comb' $K_B = 0.1\pi$ determines the plane wave component with the longest wavelength (bold numbers in Table 1). If one defines phase velocity $v_{\mathrm{ph}} = \omega/K_B$ based on $K_B = 0.1\pi$, then phase velocity is positive and, since the Poynting vector was found to be negative, one has a backward wave.

However, the amplitude of the $K_B = 0.1\pi$ harmonic ($e_0 \approx 0.174$) is much smaller than that of the $K_B - \kappa_0 = -1.9\pi$ wave (sans-serif typeface in the Table). A common convention (P. Yeh [53], B. Lombardet *et al.* [14]) is to use this highest-amplitude component as a basis for defining phase velocity. If this convention is accepted in our present example, then phase velocity becomes negative and the wave is a forward one (since the Poynting vector is also negative).

One may then wonder what the value of phase velocity "really" is. This question is not a *mathematically* sound one, as one cannot truly argue about mathematical definitions. From the physical viewpoint, however, two aspects of the notion of phase velocity are worth considering.

First, boundary conditions at the interface between two *homogeneous* media are intimately connected with the values of phase velocities and indexes of refraction (defined for homogeneous materials in the usual unambiguous sense). Fundamentally, however, it is the wave vectors in both media that govern wave propagation, and it is the continuity of its tangential component that constrains the fields. Phase velocity plays a role only due to its direct connection with the wavenumber. For periodic structures, there is not one but a whole 'comb' of wavenumbers that all need to be matched at the interface. We shall return to this subject later.

Second, in many practical cases phase velocity can be easily and clearly visualized. As an example, Fig. 7 shows two snapshots, at $t = 0$ and $t = 0.5$, of the second Bloch mode described above. For the visual clarity of this figure, low-pass filtering has been applied – without that filtering, the rightward motion of the wave is obvious in the animation but is difficult to present in static pictures. The Bloch wavenumber in the first Brillouin zone in this example is $K_B = 0.1\pi$ and the corresponding second eigenfrequency is $\omega \approx 4.276$. The phase velocity – if defined via the first Brillouin zone wavenumber – is $v_{\mathrm{ph}} = \omega/K_B \approx 4.276/0.1\pi \approx 13.61$. Over the time interval $t = 0.5$ between the snapshots, the displacement of the wave consistent with this phase velocity is $13.61 \cdot 0.5 \approx 6.8$. This corresponds quite accurately to the actual displacement in Fig. 7, proving that the first Brillouin zone wavenumber is indeed relevant to the perceived visual motion of the Bloch wave.

So, what is one to make of all this? The complete representation of a Bloch wave is given by a comb of wavenumbers $K_B - m\kappa_0$ and the respective amplitudes e_m of the Fourier harmonics. Naturally, one is inclined to distill this theoretically infinite set of data to just a few parameters that include the Poynting vector, phase and group velocities. While the Poynting vector and group velocity for the wave are rigorously and unambiguously defined, the same is *in general* not true for phase velocity.

However, there are practical cases where phase velocity is meaningful. The situation is most clear-cut when the Bloch wave has a strongly dominant long-wavelength component. Then the Bloch wave is, in a sense, close to a pure plane wave, but non-trivial effects may still arise. Even though the amplitudes of the
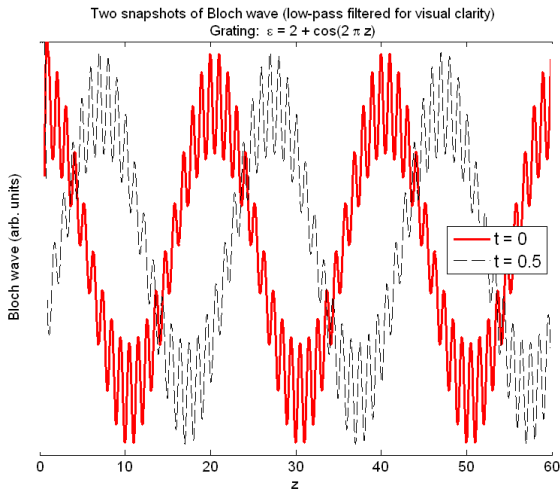
Figure 7: Two snapshots, at $t = 0$ and $t = 0.5$, of the second Bloch mode. (Low-pass filtering applied for visual clarity.) The wave moves to the right with phase velocity corresponding to the smallest positive Bloch wavenumber $K_B = 0.1\pi$.

individual higher-order harmonics may be small, it is possible for their *collective effect* to be significant. In particular, as the example in this Section has shown, the higher harmonics taken together may carry more energy than the dominant component, and in the opposite direction. In this case one has a backward wave, where phase velocity is defined by the dominant long-wavelength harmonic, while the Poynting vector is due to a collective contribution of all harmonics.

Here is a modest proposal for defining phase velocity in a more general situation. The rationale is that the motion of the wave as a whole is governed primarily by long-wavelength components; short-wavelength harmonics appear as high-frequency noise on top of a waveform with low spatial frequency. It seems appropriate, therefore, to define the 'weighted phase velocity' as

$$v_{\text{ph, weighted}} \equiv \omega \sum_{m=-\infty}^{\infty} (K_B - m\kappa_0)^{-1} |e_m|^2, \quad \|\underline{e}\|_2 = 1$$

(38)

where the $m = 0$ term is omitted if $K_B = 0$. The weighting factors $|K_B - m\kappa_0|^{-1}$ correspond to integral averaging of the wave over the spatial period. This definition may have mathematical advantages as well, as it can be written in terms of matrix-vector operations involving the diagonal matrix $\mathcal{K}$ of (27).

An alternative generalization of phase velocity in 1D is the velocity v_{field} of points with a fixed magnitude of the E field. From the zero differential

$$dE = \frac{\partial E}{\partial x} dx + \frac{\partial E}{\partial t} dt = 0$$

one obtains

$$v_{\text{field}} = \frac{dx}{dt} = -\frac{\partial E}{\partial x} \Big/ \frac{\partial E}{\partial t}$$

Unfortunately, this definition does not generalize easily to 2D and 3D, where an analogous velocity would be a tensor quantity (a separate velocity vector for each Cartesian component of the field).

For illustration and further investigation, it is convenient to have a specific example in mind (however, the analysis and conclusions will be general). As such an example, consider the structure proposed by R. Gajic, R. Meisels *et al.* [8, 19]. Their photonic crystal is a 2D square lattice of alumina rods
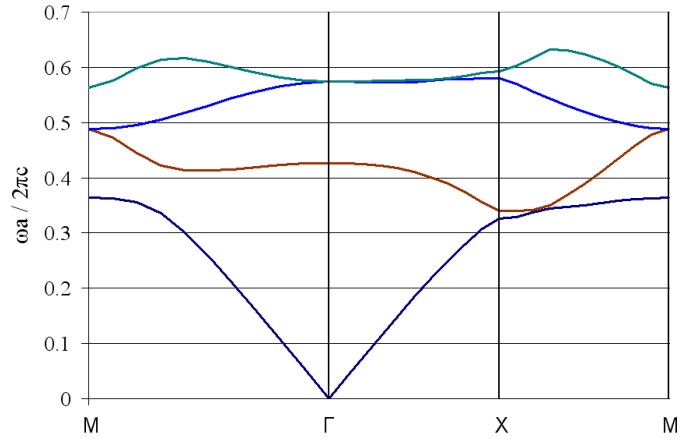

Figure 8: The H-mode band diagram of the Gajic *et al.* crystal.

($\epsilon_{\text{rod}} = 9.6$) in air. The radius of the rod is $r_{\text{rod}} = 0.61$ mm, the lattice constant $a = 1.86$ mm, so that $r/a \approx 0.33$. The length of the rods is 50 mm. Gajic, Meisels *et al.* study various cases of wave propagation and refraction. In the context of our analysis, of most interest is negative refraction for small Bloch numbers in the second band of the H-mode (TE-mode). The band diagram, computed using the plane wave method with 441 waves for the H-mode, appears in Fig. 8 and, apart from the scaling factors, is very close to the one provided by Gajic *et al.*

The TE2 dispersion curve is mildly convex around the Γ point ($K_B = 0$, $\omega a/(2\pi c) \approx 0.427$), indicating a negative second derivative $\partial^2 \omega/\partial K_B^2$ and hence a negative group velocity for small positive K_B and a possible backward wave. As we are now aware, an additional condition for a backward wave must also be satisfied: the plane-wave component corresponding to the small positive Bloch number must be appreciable (or better yet, dominant). Let us therefore consider the plane wave composition of the Bloch wave.

The amplitudes of the plane-wave harmonics for the Gajic *et al.* crystal are shown in Fig. 9. For $K_B = 0$ (i.e. at Γ) the spectrum is symmetric and characteristic of a standing wave. As K_B becomes positive and increases, the spectrum gets skewed, with the backward components ($K < 0$) increasing and the forward ones decreasing. The amplitudes of the spatial harmonics of this Bloch wave in the first Brillouin zone are quite small. It is therefore debatable whether a valid phase velocity can be attributed to this wave.

The distribution of Poynting components of the same wave and for the same set of values of the Bloch wavenumber is shown in Fig. 10. It is clear from the figure that the negative components outweigh the positive ones, so power flows in the negative direction.

IX   ARE THERE TWO SPECIES OF NEGATIVE REFRACTION?

The following argument indicates that negative refraction disappears in the homogenization limit when the size of the lattice cells tends to zero, provided that other physical parameters, including frequency, are fixed.

It is natural to normalize the coordinates as $\tilde{x} = x/a$, $\tilde{y} = y/a$, $\tilde{z} = z/a$, so that in the tilde-coordinates the 2D / 3D problem is set up in the unit square / cube and the governing equations
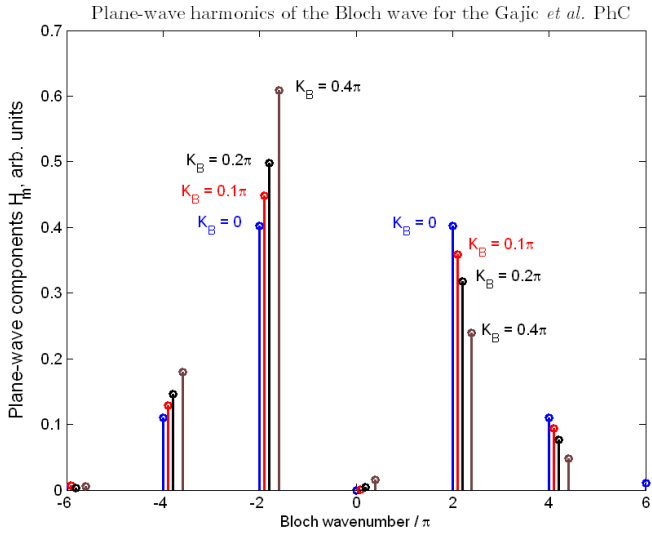
Figure 9: Amplitudes h_m of the plane-wave harmonics for the Gajic *et al.* crystal (arb. units). Second H-mode (TE2) near the Γ point on the $\Gamma \to X$ line.
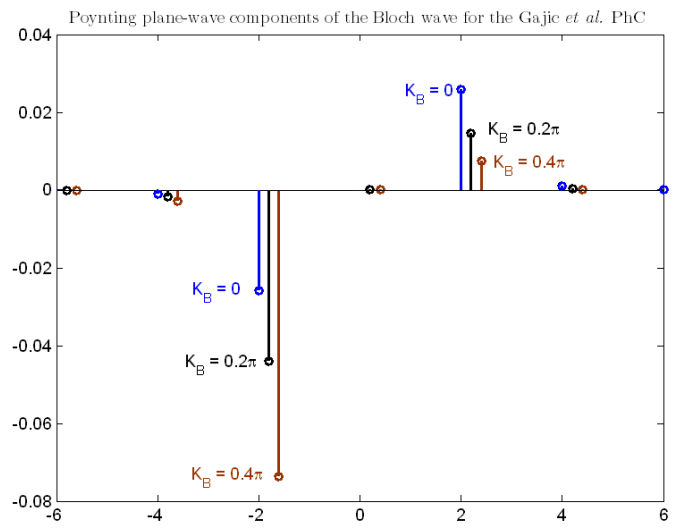

Figure 10: The plane-wave Poynting components P_m for the Gajic *et al.* crystal (arb. units). Second H-mode (TE2) near the Γ point on the $\Gamma \to X$ line.

become, in 2D and 3D, respectively,

$$\tilde{\nabla}^2 E \;+\; \tilde{\omega}^2 \mu_r \epsilon_r E \;=\; 0, \tag{39}$$

$$\tilde{\omega} = \frac{\omega a}{c} \;=\; k_0 a \;=\; 2\pi \frac{a}{\lambda_0}$$

$$\tilde{\nabla} \times \tilde{\nabla} \times \mathbf{E} \;=\; \tilde{\omega}^2 \mu_0 \epsilon(\mathbf{r}) \mathbf{E} \tag{40}$$

$$\tilde{\nabla} \times \gamma(\mathbf{r}) \tilde{\nabla} \times \mathbf{H} \;=\; \tilde{\omega}^2 \mu_0 \mathbf{H} \tag{41}$$

where c, k_0, λ_0 are the speed of light, the wavenumber and the wavelength in a vacuum. The relative permeability and permittivity μ_r and ϵ_r are periodic functions of coordinates. The homogenization limit is obtained by considering the small cell size – long wavelength limit $a \to 0$, $\tilde{K}_B = K_B a \to 0$.[12] As these limits are taken, the problem and the dispersion curves *in the normalized coordinates* remain unchanged, and the reference point $(\tilde{\omega}, \tilde{\mathbf{K}})$ approaches the origin along a fixed dispersion curve – the acoustic branch. In the example of Fig. 8, the acoutic branch is clearly identifiable as two approximately straight lines originating from the Γ point.

Around the Γ point, phase velocity in any given direction $\hat{l}$, $\omega/K_l = \tilde{\omega}/\tilde{K}_l$ is well defined and equal to group velocity $\partial\omega/\partial K_l$ simply by definition of the derivative. No backward waves can be supported in this regime. This argument suggests that the relative cell size a/λ_0 of a periodic structure with backward waves must lie above a certain threshold. To the best of my knowledge, this question is currently open and has not even been posed explicitly in the literature.

The existence of a lower bound on the cell size *for photonic crystals* is unsurprising, as they are expected to have features not much smaller than the wavelength in any event. For metamaterials, the situation is more interesting, and the cell size limit has a physical explanation. Indeed, the principal component of artificial metamaterials with negative refraction is some resonating element [45, 43, 33, 36], and the resonance frequency is, roughly, inverse proportional to size (S. Linden *et al.* [13], S. Tretyakov [48]). As the size of the lattice cell diminishes, the operating frequency *increases*, so that it is not the absolute

frequency ω but the normalized quantity $\tilde{\omega}$ that remains (approximately) constant. If the absolute frequency were to be fixed as the cell size decreases, the resonance would peter out and the backward waves would disappear, in accord with the general argument above.

The first step toward a more rigorous analysis is a working definition of negative refraction *in a metamaterial*, as opposed to a photonic crystal. The rationale for the following set of conditions is to make the Bloch wave in a metamaterial resemble, to the extent possible, a plane wave in an ideal "Veselago medium":

1. The Bloch wave in the metamaterial is, in some sense, close to a long-wavelength plane wave.

2. In particular, the plane-wave component in the first Brillouin zone has an appreciable magnitude. It is this component that defines the phase velocity of the Bloch wave.

3. Other plane-wave components collectively produce energy flow at an obtuse angle with phase velocity.

4. At the air-material interface, it is *the long-wavelength, first-Brillouin-zone*, component that serves as the excitation channel for the Bloch wave.

By this definition, the metamaterial regime corresponds to small values of $\tilde{K}_B$ ($\tilde{K}_B = K_B a \ll \pi$). Larger values of $\tilde{K}_B$ indicate a photonic crystal or grating regime, where the lattice size is comparable with the wavelength in a vacuum. Our mathematical analysis is therefore focused on the limiting case $K_B \to 0$. Further, only the case of small losses at the operating frequency is of practical interest; large losses would quench all propagating modes.[13]

In the absence of losses, ϵ is real and may be positive or negative. The estimates below depend on the average value of ϵ over the lattice cell, or equivalently on the Fourier coefficient $\tilde{\epsilon}_0$. It will be assumed that this average value is *not* close to zero;

this assumption covers the majority of practically useful situations.[14] The case $\tilde{\epsilon}_0 = 0$ is mathematically quite involved and will be considered elsewhere.

To establish a lower bound for the cell size of a "negative-index metamaterial," we first turn to the 1D case where the mathematical analysis is simpler. The E field in the normalized coordinate is represented via Fourier harmonics as

$$E(\tilde{x}) = \sum_{m \in \mathbb{Z}} e_m \exp(\mathrm{i} 2\pi m \tilde{x}) \tag{42}$$

Remark 1. Real-space (as opposed to Fourier-space) analysis is not included in this paper but can also be carried out and may in fact be more straightforward, particularly for vector fields.

The E-field equation in the Fourier domain is[15]

$$(\tilde{K}_B - 2\pi n)^2 e_n = \tilde{\omega}^2 \sum_{m \in \mathbb{Z}} \tilde{\epsilon}_{n-m} e_m \tag{43}$$

or in matrix-vector form

$$\mathcal{K}^2 \underline{e} = \tilde{\omega}^2 \mathcal{E} \underline{e}, \tag{44}$$

$$\mathcal{K}_n = \tilde{K}_B - 2\pi n; \quad \mathcal{E}_{nm} = \tilde{\epsilon}_{n-m}$$

We are interested in small eigenvalues $\tilde{\omega}^2$. Obviously, $\tilde{\omega}^2 = 0$ is an eigenvalue, with the corresponding constant field as the eigenmode. Now let $\tilde{\omega}^2 > 0$. The equation for $n = 0$ degenerates into an algebraic constraint on the harmonic amplitudes e_m ($m \neq 0$). For $\tilde{\epsilon}_0 \neq 0$ (see comments above), this constraint can be used to algebraically eliminate e_0 from the eigensystem, leading to the Schur-complement matrix problem[16]

$$\tilde{\mathcal{E}}_\varnothing \underline{e}_\varnothing = \eta \mathcal{K}_\varnothing^2 \underline{e}_\varnothing, \quad \eta \equiv \tilde{\omega}^{-2}$$

where symbol '$\varnothing$' indicates that the zeroth entry has been removed; e.g. $\underline{e}_\varnothing \equiv (\ldots, e_{-2}, e_{-1}, e_1, e_2, \ldots)$, etc. The entries of the Schur-modified matrix $\tilde{\mathcal{E}}$ are

$$\tilde{\mathcal{E}}_{\varnothing nm} = \mathcal{E}_{nm} - \tilde{\epsilon}_0^{-1} \mathcal{E}_{n0} \mathcal{E}_{0m} = \tilde{\epsilon}_{n-m} - \tilde{\epsilon}_0^{-1} \tilde{\epsilon}_n \tilde{\epsilon}_{-m}$$

The generalized eigenvalue problem $\tilde{\mathcal{E}} \underline{e}_\varnothing = \eta \mathcal{K}_\varnothing^2 \underline{e}_\varnothing$ is equivalent to the regular one with the matrix $\hat{\mathcal{E}} = \mathcal{K}_\varnothing^{-1} \tilde{\mathcal{E}}_\varnothing \mathcal{K}_\varnothing^{-1}$;

$$\hat{\mathcal{E}}_{nm} = \frac{\tilde{\epsilon}_{n-m} - \tilde{\epsilon}_0^{-1} \tilde{\epsilon}_n \tilde{\epsilon}_{-m}}{(\tilde{K}_B - 2\pi n)(\tilde{K}_B - 2\pi m)}$$

In the 'metamaterial regime' $K_B \ll 1$,

$$\hat{\mathcal{E}}_{nm} \approx \frac{\tilde{\epsilon}_{n-m} - \tilde{\epsilon}_0^{-1} \tilde{\epsilon}_n \tilde{\epsilon}_{-m}}{4\pi^2 nm}, \quad m, n = \pm 1, \pm 2, \ldots$$

The eigenvalue η is bounded by the Frobenius norm of $\hat{\mathcal{E}}$:

$$|\eta|^2 \leq \|\hat{\mathcal{E}}\|_F^2 = \sum \sum_{m,n = \pm 1, \pm 2, \ldots} \frac{|\tilde{\epsilon}_{n-m} - \tilde{\epsilon}_0^{-1} \tilde{\epsilon}_n \tilde{\epsilon}_{-m}|^2}{(4\pi^2 nm)^2}$$

$$\leq \frac{2 \cdot 4}{24^2} |\epsilon|_{\max}^2 \left(1 + |\tilde{\epsilon}_0|^{-2} |\epsilon|_{\max}^2\right)$$

---

[14] The 'effective' ϵ of the double-negative medium, assuming that this value can be adequately defined [44], should of course be negative; but it does not have to be equal to $\tilde{\epsilon}_0$.

[15] In this paper, symbol n denotes the Fourier harmonic number and is never used as index of refraction, so no confusion should arise.

[16] Infinite algebraic systems are here treated as if they were finite, with the usual techniques of linear algebra applied. This is justifiable because the original system can always be truncated to any arbitrarily large number of harmonics; since the results do not depend on that number, they are also true in the limit of the infinite system.

where it has been noted that $\sum_{n=1}^{\infty} n^{-2} = \pi^2/6$; the factor of 4 is due to summation for both positive and negative n, m. Thus the following lower bound on $\tilde{\omega}$ is established in 1D:

$$\tilde{\omega}^2 = \eta^{-1} \geq \frac{6\sqrt{2}}{|\epsilon|_{\max} \sqrt{1 + |\tilde{\epsilon}_0|^{-2} |\epsilon|_{\max}^2}} \tag{45}$$

the relative lattice cell size being $a/\lambda_0 = \tilde{\omega}/2\pi$.

Remark 2. Real-space calculation, alluded to in *Remark 1*, yields $\tilde{\omega}^2 \geq 4\pi^2 |\epsilon|_{\max}^{-1} (1 + |\tilde{\epsilon}_0|^{-1} |\epsilon|_{\max})^{-1}$. This is a stronger inequality than (45); the latter can be improved if the crude estimate of the Fourier coefficients $|\tilde{\epsilon}_n| < |\epsilon|_{\max}$ is replaced with a more accurate one (the coefficients decay as n increases).

As a separate but related matter, it is also instructive to examine the direction of power flow. The average Poynting vector is, according to (23) and with convenient normalization,

$$\tilde{P} \equiv 2\omega\mu_0 < P > = K_B |e_0(K_B)|^2 +$$

$$\sum_{m=1}^{\infty} (K_B - 2\pi m) |e_m(K_B)|^2 + (K_B + 2\pi m) |e_{-m}(K_B)|^2 \tag{46}$$

Here it is essential to indicate explicitly that the Fourier amplitudes e_m depend on the Bloch parameter K_B. Since the waves corresponding to $\pm K_B$ are, in the lossless case (real ϵ), complex conjugates of one another, we have $e_{-m}(K_B) = e_m^*(-K_B)$, and the expression for the Poynting vector becomes

$$\tilde{P} = K_B |e_0(K_B)|^2 + \sum_{m=1}^{\infty} (K_B - 2\pi m) |e_m(K_B)|^2$$

$$+ (K_B + 2\pi m) |e_m(-K_B)|^2$$

$$= K_B |e_0(K_B)|^2 + K_B \sum_{m=1}^{\infty} (|e_m(K_B)|^2 + |e_m(-K_B)|^2)$$

$$- 2\pi \sum_{m=1}^{\infty} m(|e_m(K_B)|^2 - |e_m(-K_B)|^2) \tag{47}$$

The first two terms in (47) are directly proportional to K_B. To make this small parameter explicit in the third sum as well, we may write

$$\tilde{P} = K_B \left[|e_0|^2 + \sum_{m=1}^{\infty} (|e_m(K_B)|^2 + |e_m(-K_B)|^2) - 2\pi \sum_{m=1}^{\infty} m \frac{\partial e_m^2}{\partial K_B} \right] \tag{48}$$

For small $\tilde{\omega}$, the expression in the big brackets tends to be dominated by $|e_0|^2$ and to be positive, making the backward-wave phenomenon difficult to achieve. Indeed, the zero-order harmonic is normally dominant because the eigenproblem (43) for small $\tilde{\omega}$ constrains the values of all Fourier harmonics *with the exception of* e_0:

$$|e_n| = \tilde{\omega}^2 (\tilde{K}_B - 2\pi n)^{-2} \left| \sum_{m \in \mathbb{Z}} \epsilon_{n-m} e_m \right|$$

$$\leq \tilde{\omega}^2 (\tilde{K}_B - 2\pi n)^{-2} \|\epsilon\|_{l_2} \|e\|_{l_2}, \quad n \neq 0 \tag{49}$$

2D analysis proceeds in the same manner as in 1D, but some changes need to be highlighted. The E-field equation in the Fourier domain is

$$|\tilde{\mathbf{K}}_B - 2\pi\mathbf{n}|^2 e_\mathbf{n} = \tilde{\omega}^2 \sum_{\mathbf{m} \in \mathbb{Z}^2} \tilde{\epsilon}_{\mathbf{n}-\mathbf{m}} e_\mathbf{m}, \quad \forall \mathbf{n} \in \mathbb{Z}^2 \tag{50}$$

The focus again is on the 'metamaterial regime' with a small K_B. For $K_B = 0$, $\tilde{\omega}^2 = 0$ is an eigenvalue, with the corresponding constant-field eigenmode. As in 1D, for nonzero $\tilde{\omega}$, the equation for $\mathbf{n} = 0$ imposes an algebraic constraint on $e_{\mathbf{m}}$ ($\mathbf{m} \neq 0$). The Schur-complement matrix problem has the same generic form as before:

$$\tilde{\mathcal{E}}\underline{e}_\varnothing = \eta \mathcal{K}_\varnothing^2 \underline{e}_\varnothing \tag{51}$$

where the entries of $\tilde{\mathcal{E}}$ are

$$\tilde{\mathcal{E}}_{\mathbf{nm}} = \mathcal{E}_{\mathbf{nm}} - \tilde{\epsilon}_0^{-1} \mathcal{E}_{\mathbf{n}0}\mathcal{E}_{0\mathbf{m}} = \tilde{\epsilon}_{\mathbf{n-m}} - \tilde{\epsilon}_0^{-1}\tilde{\epsilon}_{\mathbf{n}}\tilde{\epsilon}_{-\mathbf{m}}$$

Here some sequential numbering scheme for the integer vectors $\mathbf{n} \in \mathbb{Z}^2$ is implied, so that subscripts $\mathbf{n}$, $\mathbf{m}$ refer to the row / column of the matrix corresponding to $\mathbf{n}$, $\mathbf{m}$.

As in 1D, the generalized eigenvalue problem (51) is equivalent to the regular one with the matrix $\hat{\mathcal{E}} = \mathcal{K}_\varnothing^{-1}\tilde{\mathcal{E}}_\varnothing\mathcal{K}_\varnothing^{-1}$. For $K_B = 0$,

$$\hat{\mathcal{E}}_{\mathbf{nm}} = \frac{\tilde{\epsilon}_{\mathbf{n-m}} - \tilde{\epsilon}_0^{-1}\tilde{\epsilon}_{\mathbf{n}}\tilde{\epsilon}_{-\mathbf{m}}}{4\pi^2 nm}$$

where $n = |\mathbf{n}| \neq 0$, $m = |\mathbf{m}| \neq 0$ (by definition, the Schur-modified matrix does not contain the 'zeroth' row and column). The Frobenius norm of $\hat{\mathcal{E}}$ again provides a bound for the eigenvalue η:

$$|\eta|^2 \leq \|\hat{\mathcal{E}}\|_F^2 = \sum\sum_{\mathbf{m},\mathbf{n}\in\mathbb{Z}^2}^* \frac{|\tilde{\epsilon}_{\mathbf{n-m}} - \tilde{\epsilon}_0^{-1}\tilde{\epsilon}_{\mathbf{n}}\tilde{\epsilon}_{-\mathbf{m}}|^2}{(4\pi^2 nm)^2} \tag{52}$$

The asterisk indicates that the terms with a zero denominator are omitted. To evaluate the double sum, one needs a more accurate estimate of the Fourier coefficients than in 1D. Let

$$|\tilde{\epsilon}_{\mathbf{n}}| = \left| \int_{[0,1]\times[0,1]} \epsilon(\tilde{\mathbf{r}}) \exp(\mathrm{i}2\pi\mathbf{n}\cdot\tilde{\mathbf{r}})\, d\Omega \right| \leq \frac{g}{n} \tag{53}$$

where g is independent of n but does depend on the distribution of ϵ in the lattice cell. For example, integration by parts yields

$$g \leq \frac{\|\tilde{\nabla}\epsilon\|_{L1}}{2\pi}, \quad \text{where } \|\tilde{\nabla}\epsilon\|_{L1} \equiv \int_{[0,1]\times[0,1]} |\tilde{\nabla}\epsilon|\, d\Omega$$

Here $\tilde{\nabla}\epsilon$ is understood in the sense of distributions and includes surface delta-functions corresponding to the jumps of ϵ (if any).

Substituting the upper bound (53) for the Fourier coefficients into the Frobenius norm estimate (52) yields, after some algebraic manipulation,

$$|\eta|^2 \leq \|\hat{\mathcal{E}}\|_F^2 \leq 2\frac{1}{(4\pi^2)^2}\left[g^2 s_1 + \tilde{\epsilon}_0^{-2}g^4 s_2 + \tilde{\epsilon}_0^2 s_3\right] \tag{54}$$

where s_{1-3} are the following sums:

$$s_1 = \sum\sum_{\mathbf{m},\mathbf{n}\in\mathbb{Z}^2}^* \frac{1}{n^2 m^2 |\mathbf{n}-\mathbf{m}|^2} \approx 34.8$$

$$s_2 = \sum\sum_{\mathbf{m},\mathbf{n}\in\mathbb{Z}^2}^* \frac{1}{n^4 m^4} = s_3^2 \approx 27.2$$

$$s_3 = \sum\sum_{\mathbf{n}\in\mathbb{Z}^2}^* \frac{1}{n^4} \approx 5.2$$

As before, the normalized lattice cell size $a/\lambda_0 = \tilde{\omega}/2\pi$, with $\tilde{\omega}^2 = 1/\eta$.

As an illustrative example, let us apply this result to a lattice of cylindrical rods of radius $r_{\rm rod}$ and permittivity $\epsilon_{\rm rod}$. A simple explicit expression for the Fourier amplitudes $\tilde{\epsilon}$ in this case is

available (see e.g. K. Sakoda [34], p. 25), and so parameter g can also be evaluated explicitly:

$$\tilde{\epsilon}_{\mathbf{n}} = 2v(\epsilon_{\rm rod} - 1)\frac{J_1(n\tilde{r}_{\rm rod})}{n\tilde{r}_{\rm rod}}; \quad v = \frac{\pi r_{\rm rod}^2}{a^2}, \quad \tilde{r}_{\rm rod} = \frac{2\pi r_{\rm rod}}{a}$$

where J_1 is the Bessel function, v is the fraction of the volume occupied by the cylinder, and $\tilde{r}_{\rm rod}$ is its normalized radius. The Fourier coefficients decay even faster than our minimum requirement of $\sim 1/n$ because J_1 decays, asymptotically in inverse proportion with the square root of n. Estimating J_1 very roughly just by its maximum value of ~ 0.6, we get

$$g \leq 2v|\epsilon_{\rm rod} - 1|\frac{0.6}{\tilde{r}_{\rm rod}} = \frac{0.6 r_{\rm rod}|\epsilon_{\rm rod} - 1|}{a} \leq 0.6|\epsilon_{\rm rod} - 1| \tag{55}$$

For a numerical illustration, let us evaluate the lower bound for the lattice cell in the Gajic *et al.* crystal presented earlier. For $\epsilon_{\rm rod} = 9.6$, equation (55) gives $g \approx 5.16$. Since the volume fraction is $v \approx 0.338$, the average value of ϵ is $\tilde{\epsilon}_0 \approx 3.91$, and from (54) $\eta \leq 1.71$. Then $\tilde{\omega}^2 = 1/\eta \geq 0.87$ and the normalized cell size $a/\lambda_0 = \tilde{\omega}/2\pi \geq 0.14$. In reality, negative refraction in this crystal is observed above ~ 68 GHz, which corresponds to $\lambda_0 \leq 4.4$ mm and $a/\lambda_0 \geq 0.42$, comfortably above the theoretical lower bound of 0.14.

If rods were made of an (ideal) plasmonic material with $\epsilon = -2$ (losses neglected), the same calculation would produce a smaller bound on the cell size, $a/\lambda_0 \gtrsim 0.06$. Needless to say, (54) is only a *necessary* condition for negative refraction and is very far from being sufficient. This condition makes it *possible* for the higher-order Fourier harmonics of the Bloch wave to outweigh the first-Brilloin-zone harmonic, but does not guarantee that they will do so and that they will have the desirable sign.

X Summary

1. The history of backward waves and negative-index materials can be traced back to the beginning of the 20$^{\rm th}$ century (H. Lamb, A. Schuster, H.C. Pocklington) and to the work of Russian physicists (L.I. Mandelshtam, D.V. Sivukhin, V.E. Pafomov, R.A. Silin, V.G. Veselago) in the 1940s–1970s. Since the experimental demonstration by D.R. Smith and the discovery of the 'perfect lens' phenomenon by J.B. Pendry in 2000, there has been an explosion of interest in negative refraction and backward waves in periodic structures.

2. The Fourier-Bloch decomposition of the field into plane-wave components clarifies the nature of backward waves. Phase velocity is governed primarily by the first-Brillouin-zone component of the Bloch wave – assuming that this component has an appreciable magnitude. In contrast, energy flow is a *collective effect* of all plane-wave harmonics. Backward waves occur when higher-order harmonics, taken together, outweigh the first one and have the opposite sign.

3. *Intrinsic* and *extrinsic* characteristics should be distinguished. The forward or backward character of a wave is its intrinsic characteristic in the bulk of the material. At interface boundaries, the Bloch wave can in principle be excited via any of its plane-wave components. The type of refraction depends on both factors: the intrinsic character of the wave and the 'excitation channel'.

4. Negative-index media are usually subdivided into two kinds: 'metamaterials,' typically containing relatively small

resonating elements within a lattice cell, and 'photonic crystals' – periodic dielectric structures such as arrays of dielectric cylinders, spheres, etc. Consequently, negative refraction is usually classified as two species: one occurring in metamaterials, another one in photonic crystals.

5. Metamaterials might seem to approximate, in the limiting case of a small cell, an ideal double-negative 'Veselago medium' supporting backward waves. However, this paper argues that there is a fundamental lower limit on the lattice cell size, relative to the vacuum wavelength, for a periodic dielectric medium capable of supporting backward waves. As the cell size tends to zero, the operating point on the normalized band diagram of the structure falls on the acoustic branch, thereby eliminating the difference between phase and group velocities. The paper provides explicit lower bounds for the cell size.

6. In short, there are fundamental limitations on how small the lattice size can be for negative index materials. The "Veselago medium" may not in fact be realizable as a limiting case of spatially periodic dielectric structures with a small cell size.

ACKNOWLEDGMENT

XI   REFERENCES

[1] P.A. Belov, C.R. Simovski, and S.A. Tretyakov. Backward waves and negative refraction in photonic (electromagnetic) crystals. *Journal of Communications Technology and Electronics*, 49(11):1199–1207, 2004.

[2] W. Cai, U.K. Chettiar, H.-K. Yuan, V.C. de Silva, A.V. Kildishev, V.P. Drachev, and V.M. Shalaev. Metamagnetics with rainbow colors. *Opt. Express*, 15:3333–3341, 2007.

[3] E. Cubukcu, K. Aydin, E. Ozbay, S. Foteinopolou, and C. M. Soukoulis. Subwavelength resolution in a two-dimensional photonic-crystal-based superlens. *Phys. Rev. Lett.*, 91(20):207401, Nov 2003.

[4] R.A. Depine and A. Lakhtakia. A new condition to identify isotropic dielectric-magnetic materials displaying negative phase velocity. *Microwave Opt. Technol. Lett.*, 41:315–316, 2004.

[5] G. Dolling, M. Wegener, C.M. Soukoulis, and S. Linden. Negative-index metamaterial at 780 nm wavelength. *Optics Letters*, 32(1):53–55, 2007.

[6] Gunnar Dolling, Christian Enkrich, Martin Wegener, Costas M. Soukoulis, and Stefan Linden. Low-loss negative-index metamaterial at telecommunication wavelengths. *Optics Letters*, 31(12):1800–1802, 2006.

[7] G.V. Eleftheriades and K.G. Balmain. *Negative Refraction Metamaterials: Fundamental Principles and Applications*. Wiley-IEEE Press, 2005.

[8] R. Gajic, R. Meisels, F. Kuchar, and K. Hingerl. Refraction and rightness in photonic crystals. *Opt. Express*, 13:8596–8605, 2005.

[9] Christopher L. Holloway, Edward F. Kuester, James Baker-Jarvis, and Pavel Kabos. A double negative (DNG) composite medium composed of magnetodielectric spherical particles embedded in a matrix. *IEEE Transactions on Antennas and Propagation*, 51(10):2596–2603, 2003.

[10] Andrew A. Houck, Jeffrey B. Brock, and Isaac L. Chuang. Experimental observations of a left-handed material that obeys Snell's law. *Phys. Rev. Lett.*, 90(13):137401, Apr 2003.

[11] H. Lamb. On group-velocity. *Proc. London Math. Soc.*, 1:473–479, 1904.

[12] L.D. Landau and E.M. Lifshitz. *Electrodynamics of Continuous Media*. Oxford; New York: Pergamon, 1984.

[13] Stefan Linden, Christian Enkrich, Gunnar Dolling, Matthias W. Klein, Jiangfeng Zhou, Thomas Koschny, Costas M. Soukoulis, Sven Burger, Frank Schmidt, and Martin Wegener. Photonic metamaterials: Magnetism at optical frequencies. *IEEE Journal of Selected Topics in Quantum Electronics*, 12(6):1097–1105, 2006.

[14] B. Lombardet, L. A. Dunbar, R. Ferrini, and R. Houdré. Fourier analysis of Bloch wave propagation in photonic crystals. *J. Opt. Soc. Am. B*, 22:1179–1190, 2005.

[15] Chiyan Luo, Steven G. Johnson, J. D. Joannopoulos, and J. B. Pendry. All-angle negative refraction without negative effective index. *Phys. Rev. B*, 65(20):201104, May 2002.

[16] L.I. Mandelshtam. Group velocity in crystalline arrays. *Zh. Eksp. Teor. Fiz.*, 15:475–478, 1945.

[17] L.I. Mandelshtam. *Polnoe Sobranie Trudov, v. 2*. Akademiia Nauk SSSR, 1947.

[18] L.I. Mandelshtam. *Polnoe Sobranie Trudov, v. 5*. Akademiia Nauk SSSR, 1950.

[19] R. Meisels, R. Gajic, F. Kuchar, and K. Hingerl. Negative refraction and flat-lens focusing in a 2d square-lattice photonic crystal at microwave and millimeter wave frequencies. *Opt. Express*, 14:6766–6777, 2006.

[20] P.W. Milonni. *Fast Light, Slow Light and Left-Handed Light*. Taylor & Francis, 2004.

[21] Graeme W. Milton and Nicolae-Alexandru P. Nicorovici. On the cloaking effects associated with anomalous localized resonance. *Proc. R. Soc. Lond. A*, 2006.

[22] Graeme W. Milton, Nicolae-Alexandru P. Nicorovici, Ross C. McPhedran, and Viktor A. Podolskiy. A proof of superlensing in the quasistatic regime, and limitations of superlenses in this regime due to anomalous localized resonance. *Proc. R. Soc. Lond. A*, 461(2064):3999–4034, Dec 2005.

[23] R. Moussa, S. Foteinopoulou, Lei Zhang, G. Tuttle, K. Guven, E. Ozbay, and C. M. Soukoulis. Negative refraction and superlens behavior in a two-dimensional photonic crystal. *Physical Review B (Condensed Matter and Materials Physics)*, 71(8):085106, 2005.

[24] N.A. Nicorovici, R.C. McPhedran, and G.W. Milton. Optical and dielectric properties of partially resonant composites. *Phys. Rev. B*, 49(12):8479–8482, Mar 1994.

[25] M. Notomi. Theory of light propagation in strongly modulated photonic crystals: Refractionlike behavior in the vicinity of the photonic band gap. *Phys. Rev. B*, 62(16):10696–10705, Oct 2000.

[26] V.E. Pafomov. K voprosu o perehodnom izluchenii i izluchenii Vavilova-Cherenkova. *Zh. Eksp. Teor. Fiz.*, 36(6):1853–1858, 1959.

[27] C. G. Parazzoli, R. B. Greegor, K. Li, B. E. C. Koltenbah, and M. Tanielian. Experimental verification and simulation of negative index of refraction using Snell's law. *Phys. Rev. Lett.*, 90(10):107401, Mar 2003.

[28] P. V. Parimi, W. T. Lu, P. Vodo, J. Sokoloff, J. S. Derov, and S. Sridhar. Negative refraction and left-handed electromagnetism in microwave photonic crystals. *Physical Review Letters*, 92(12):127401, 2004.

[29] J.B. Pendry. Negative refraction makes a perfect lens. *Phys. Rev. Lett.*, 85(18):3966–3969, Oct 2000.

[30] J.B. Pendry, A.J. Holden, D.J. Robbins, and W.J. Stewart. Magnetism from conductors and enhanced nonlinear phenomena. *IEEE Transactions on Microwave Theory and Techniques*, 47(11):2075–2084, Nov 1999.

[31] J.B. Pendry and D.R. Smith. Reversing light with negative refraction. *Phys. Today*, 57:37–43, 2004.

[32] H.C. Pocklington. Growth of a wave-group when the group velocity is negative. *Nature*, 71:607–608, 1905.

[33] S. Anantha Ramakrishna. Physics of negative refractive index materials. *Rep. Prog. Phys.*, 68:449–521, 2005.

[34] Kazuaki Sakoda. *Optical Properties of Photonic Crystals*. Berlin; New York: Springer, 2005.

[35] A. Schuster. *Introduction to the Theory of Optics*. Edward Arnold, London, 1904.

[36] Vladimir M. Shalaev. Optical negative-index metamaterials. *Nature Photonics*, 1:41–48, 2006.

[37] R.A. Shelby, D.R. Smith, and S. Schultz. Experimental verification of a negative index of refraction. *Science*, 292(5514):77–79, 1990.

[38] R.A. Silin. Waveguiding properties of two-dimensional periodical slow-wave systems. *Voprosy Radioelektroniki, Elektronika*, 4:11–33, 1959.

[39] R.A. Silin. Optical properties of artificial dielectrics. *Izvestia VUZov Radiofizika*, 15:809–820, 1972.

[40] D.V. Sivukhin. The energy of electromagnetic waves in dispersive media. *Optika i Spektroskopia*, 3:308–312, 1957.

[41] Daniel Sjöberg. Homogenization of dispersive material parameters for Maxwell's equations using a singular value decomposition. *Multiscale Modeling & Simulation*, 4(3):760–789, 2005.

[42] Daniel Sjöberg, Christian Engstrom, Gerhard Kristensson, David J. N. Wall, and Niklas Wellander. A Floquet–Bloch decomposition of Maxwell's equations applied to homogenization. *Multiscale Modeling & Simulation*, 4(1):149–171, 2005.

[43] D. R. Smith and D. C. Vier. Design of metamaterials with negative refractive index. In M. Razeghi and G. J. Brown, editors, *Quantum Sensing and Nanophotonic Devices. Edited by Razeghi, Manijeh; Brown, Gail J. Proceedings of the SPIE, Volume 5359, pp. 52-63 (2004).*, pages 52–63, 2004.

[44] David R. Smith and John B. Pendry. Homogenization of metamaterials by field averaging. *Journal of the Optical Society of America B*, 23(3):391–403, 2006.

[45] D.R. Smith, Willie J. Padilla, D.C. Vier, S.C. Nemat-Nasser, and S. Schultz. Composite medium with simultaneously negative permeability and permittivity. *Phys. Rev. Lett.*, 84(18):4184–4187, May 2000.

[46] Mark I. Stockman. Criterion for negative refraction with low optical losses from a fundamental principle of causality. *Physical Review Letters*, 98(17):177404, 2007.

[47] S.A. Tretyakov. Research on negative refraction and backward-wave media: A historical perspective. In *Proceedings of the EPFL Latsis Symposium, Lausanne*, 2005.

[48] Sergei Tretyakov. On geometrical scaling of split-ring and double-bar resonators at optical frequencies. *Metamaterials*, 1(1):40–43, 2007.

[49] Igor Tsukerman. *Computational Methods for Nanoscale Applications: Particles, Plasmons and Waves*. Springer, 2007. (To be published.).

[50] V.G. Veselago. Electrodynamics of substances with simultaneously negative values of ϵ and μ. *Sov Phys Uspekhi*, 10(4):509–514, 1968.

[51] Mark S. Wheeler, J. Stewart Aitchison, and Mohammad Mojahedi. Coated nonmagnetic spheres with a negative index of refraction at infrared frequencies. *Physical Review B (Condensed Matter and Materials Physics)*, 73(4):045105, 2006.

[52] Vassilios Yannopapas and Alexander Moroz. Negative refractive index metamaterials from inherently non-magnetic materials for deep infrared to terahertz frequency ranges. *Journal of Physics: Condensed Matter*, 17(25):3717–3734, 2005.

[53] Pochi Yeh. Electromagnetic propagation in birefringent layered media. *J. Opt. Soc. Am.*, 69(5):742–756, 1979.

[54] R. Zengerle. Light propagation in singly and doubly periodic planar waveguides. *J. Mod. Optics*, 34:1589–1617, 1987.

[55] Shuang Zhang, Wenjun Fan, Kevin J. Malloy, Steven R.J. Brueck, Nicolae C. Panoiu, and Richard M. Osgood. Demonstration of metal-dielectric negative-index metamaterials with improved performance at optical frequencies. *J. Opt. Soc. Am. B*, 23(3):434–438, 2006.

AUTHOR'S NAME AND AFFILIATION

Igor Tsukerman, Department of Electrical and Computer Engineering, The University of Akron, OH 44325–3904, USA.
`igor@uakron.edu`